International Biodeterioration & Biodegradation 186 (2024) 105681

Contents lists available at ScienceDirect

International Biodeterioration & Biodegradation

journal homepage: www.elsevier.com/locate/ibiod

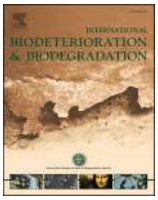

Centimetric circular areas uncolonized by microbial biofilms (CUMBs) on marble surfaces and insights on a lichen-related origin

Marta Cicardi [a], Davide Bernasconi [b], Luca Martire [b], Linda Pastero [b], Giulia Caneva [c], Sergio E. Favero-Longo [a,*]

[a] Dipartimento di Scienze della Vita e Biologia dei Sistemi, Università di Torino, Viale Mattioli 25, 10125, Torino, Italy
[b] Dipartimento di Scienze della Terra, Università di Torino, Via Valperga Caluso 35, 10125, Torino, Italy
[c] Dipartimento di Scienze, Università di RomaTre, viale Marconi 446, 00146, Roma, Italy

ARTICLE INFO

Keywords:
Allelopathy
Bioreceptivity
Calcite reprecipitation
Discolourations
Lichen secondary metabolites
Stone cultural heritage

ABSTRACT

This study investigated the poorly known phenomenon of Centimetric circular areas Uncolonized by Microbial Biofilms (CUMBs) which is frequently observed on natural and heritage stone surfaces displaying widespread lithobiontic colonization. In order to unveil a possible relationship with past lichen colonization, analyses were carried out on the distribution, morphometry, physical and mineralogical properties, and microscopic features of CUMBs on the marble surfaces of a balustrade in the Garden of a Savoy residence in Torino (Italy; UNESCO-WHS 823bis) and in its original quarry site in the W-Alps. Image analyses of CUMBs displayed a distributional and dimensional compatibility with lichen thalli (re-)colonizing surfaces in their vicinity. Invasive analyses on quarry materials displayed similar microscopic modifications in marble layers beneath CUMBs and lichens, associated to a higher stabilization of the calcite {01–12} form, which is favoured by the presence of organic substances. These findings support the hypothesis of a lichen origin for some CUMBs, which may derive from the modification of physical stone properties and/or a long-lasting allelopathic effect affecting surface bioreceptivity.

1. Introduction

Saxicolous lichens are common biodeteriogens of rocks, including the outdoor stone heritage surfaces, and their occurrence and relevance in historical sites have been described since long time (Nimis et al., 1992; Piervittori et al., 2004; Favero-Longo and Viles 2020). They usually display an epilithic growth, with their thallus mostly developing on the stone surface and some mycobiont structures penetrating the substrate. In other cases, however, they display an endolithic growth, with the thallus (including the photobiont layer) growing entirely within the rock substrate. Both these growth patterns are often associated with physical and chemical deterioration processes (de los Rìos and Souza Egipsy 2021; Pinna 2021). Physical deterioration is mostly exerted by hyphal penetration and volume changes in cyclic hydration and dehydration of thalli, which cause pressures and, as a consequence, disaggregation and detachment of mineral grains (Chen et al., 2000; Salvadori and Casanova Municchia 2016). Also, lichens secrete a huge variety of metabolites with acidic and chelating functions, supporting chemical modification of rock-forming minerals and, sometimes, dissolution processes (Seaward 2015; Gadd 2017). It is also proved that, at least in some cases, respiration-induced acidification of the substrate is sufficient to solubilize minerals (Weber et al., 2011).

Lichen colonization determines peculiar biodeterioration patterns on the rock surfaces, such as pitting (formation of sub-millimetric cavities), exfoliations, and depressions (Lombardozzi et al., 2012; Pinna 2021), which may persist as tracks even after the life of thalli (Danin and Caneva 1990; Caneva et al., 2020). Moreover, biomineral deposits (as oxalates) and traces of secondary metabolites were recognized as markers of past colonization by lichens (Edwards et al., 2003; Casanova Municchia et al., 2014; Miralles et al., 2015). For some combinations of species, lithologies, and climate conditions, however, macroscopic observations of differential erosion with and without lichen thalli, as well as chemical analyses of substrate solubilization rates, indicated that lichens can act as a physical barrier against other weathering factors and pollutants (umbrella-like protective effect) (Carter and Viles 2005; McIlroy de la Rosa et al., 2014). It was also claimed that the

* Corresponding author. Università degli Studi di Torino, Dipartimento di Scienze della Vita e Biologia dei Sistemi, Viale Mattioli 25, 10125, Torino, Italy.
E-mail addresses: marta.cicardi@unito.it (M. Cicardi), davide.bernasconi@unito.it (D. Bernasconi), luca.martire@unito.it (L. Martire), linda.pastero@unito.it (L. Pastero), giulia.caneva@uniroma3.it (G. Caneva), sergio.favero@unito.it (S.E. Favero-Longo).

https://doi.org/10.1016/j.ibiod.2023.105681
Received 29 May 2023; Received in revised form 31 August 2023; Accepted 6 September 2023
Available online 15 September 2023

precipitation of (bio-)minerals at the lichen-substrate interface, as in the case of oxalate deposits, may produce a protective shield and reduce the deterioration (Gadd and Dyer 2017). Other patterns of chemical transformation associated to hyphal penetration may also seal and reduce the effective porosity of rock substrates, contributing to a hardening and protective effect against abiotic weathering agents (Guglielmin et al., 2011; Slavík et al., 2017).

It is worth noting that biodeterioration and bioprotection processes are not mutually exclusive, and, in the case of a thallus on its substrate, they can counteract and/or combine their effects (Bungartz and Garvie,

Fig. 1. The phenomenon of CUMBs observed on different stone surfaces. (A) Marble statue in the Monumental Cemetery of Milan (Italy); (B) marble statue in Parma (Italy); (C) cement pavement, beneath a fig tree, in Saint Jean Cap-Ferrat near Nice (France); (D) cement balustrade in the Kasteel de Haar near Utrecht (Netherlands); (E) marble balustrade and (F) marble statue in the Monumental Cemetery of Milan (Italy); (G–H) sandstone pavements of the walls of Aigues-Mortes (France; G) and of the Palace of the Popes in Avignon (France; H). Arrows indicate CUMBs; # indicate lichens in the nearby (in the inset in H).

2004; Bartoli et al., 2014; Morando et al., 2017). It is thus the dynamic balance between biodeterioration and bioprotection functions that determines the final effect of a certain lichen species on a certain lithology (McIlroy de la Rosa et al., 2013, 2014). However, this also depends on the bioclimatic and (micro-)environmental conditions, with the same species potentially providing bioprotection in wet temperate environments and biodeterioration in hot dry ones (Carter and Viles 2005).

A differential biodeterioration of stone can occur not only depending on exposition, but also in the same conditions, as observed in the S-facing exposure of the limestone walls of the Church of the Virgin in Martvili (Georgia), where a differential erosion phenomenon started with a circular discoloration was observed leading progressively to the detachment of flakes of limestone at its center (Caneva et al., 2014). In such xeric conditions of the walls, the cause was referred to an endolithic penetration of cyanobacteria and meristematic fungi, which started the growth taking advantage from some endogenous discontinuities on the surfaces (Caneva et al., 2014). Furthermore, more recently, on restored marble surfaces already displaying advanced epilithic recolonization, a phenomenon of Centimetric circular areas Uncolonized by Microbial Biofilms, totally or with circular uncolonized borders and only the center colonized, was also described (Caneva et al., 2020). On the basis of historical photographic documentation and additional literature-based clues, these areas were hypothesized as tracks of past lichen colonization.

Indeed, such patterns of differential growths related to a different bioreceptivity (*sensu* Guillitte, 1995), that we propose to call CUMBs, are extremely widespread and visible in many environmental contexts, both on rock outcrops and monuments, and on different stone substrates, as marble, cement, sandstone and others (Fig. 1). In some cases, epilithic microbial absence empirically appears related to microbial endolithic growths or inhibition haloes (Fig. 1A; see also Cuberos-Cáceres et al., 2022), or to the inhibitory chemical effects of bird excrements (Fig. 1B; see also Dyer, 2017) or of some fruit dropping (Fig. 1C). In many others, the particular shape of CUMBs, and co-presence of CUMBs and lichens in the present or in the past, may support the hypothesis of a strict relationship among them (Fig. 1D–H).

Surprisingly, however, the phenomenon of CUMBs on stone surfaces, and particularly on marble, has never been quantitatively characterized and, with respect to the lichen-related origin, the processes involved are not yet clarified. In their work, Caneva et al. (2020) suggested on a bibliographic basis that certain lichen species observed in the past on the marble surfaces could have left long-lasting allelopathic substances, without excluding a potential influence of lichen-induced modifications on rock physical properties. Both these hypotheses, however, still need to be experimentally examined.

In this research, we aimed to verify the hypothesis that, at least in some cases, CUMBs on marble surfaces are related to past interactions between the carbonate substrate and lichen thalli, which may have determined physical modifications of the stone material and/or a long-term allelopathic effect, affecting its bioreceptivity. In this effort to unveil a possible lichen origin of some CUMBs, we will describe their distribution, morphometry, physical and mineralogical properties, and microscopic features. To accomplish these goals, we examined a marble balustrade in the Garden of a 17th century Residence of the Royal House of Savoy (Villa della Regina, UNESCO-WHS 823bis, Torino, NW-Italy), deeply affected by lichen and other lithobiontic recolonization, as well as by the CUMBs pattern, at approx. 20 years after the last restoration intervention. Moreover, considering that in-depth modifications of marble related to such phenomenon may be detectable only with destructive analyses, we also collected samples from one of the original quarries in W-Alps. On both the heritage and natural surfaces, CUMBs and their surrounding surfaces colonized by microbial biofilms were characterized in terms of morphometry, color, water absorption and mineralogical composition, by image analysis, colorimetry, contact sponge method and X-ray powder diffraction, respectively. For natural surfaces, the occurrence of biological structures and other characterizing features beneath the colonized and uncolonized rock surfaces was also evaluated by light, fluorescence and cathodoluminescence microscopy. Each analysis was also carried out on nearby areas currently colonized by lichens, as a comparison.

2. Materials and methods

2.1. Study sites

The CUMB phenomenon and lichen colonization were investigated at (a) the Villa della Regina (Torino, Italy; UTM ED50 32T 45°03′28.93″N 7°42′28.78″E; 300 m a.s.l.) and (b) the marble quarry of Rocca Bianca (Prali, Germanasca Valley, Torino, Italy; UTM ED50 32T 44°54′24″N 7°04′58″E; 1943 m a.s.l).

The Villa della Regina is located on the Western side of the Hill of Torino, at 1.2 Km from the Po River and 2.4 Km from the city center, lying in the Cfa climatic zone (C – temperate, f - no dry season a - hot summer, according to the Köppen Geiger climate classification; Kottek et al., 2006), with average temperatures ranging from 2.5 °C (av. min. December) to 27.9 °C (av. max. July) and average annual rainfall around 870 mm (https://webgis.arpa.piemonte.it/secure_apps/portale-sul-clima-in-piemonte/). The buildings are surrounded by different gardens, which include various architectural elements, like fountains, statues, grottos, and balustrades. Here, we focused the investigations on the sun-exposed, upper horizontal surfaces of the capstones of the first balustrade upwards the main building (Fig. 2A), limiting the western side of the Garden of Flowers, structured in two branches (northern and southern). Each branch, consisting of a straight and a curved part, includes six and three modules (approx. 3.6 × 0.3 m), respectively, of columnar balusters covered by a capstone and delimited by two pillars. The balustrade was severely damaged during second world war and, thus, partially reassembled in early 1950s. Before the public opening of the Villa in 2007, after decades of abandonment, stone surfaces of the Garden underwent restoration, including the examined balustrade in summer 2003. The main capstone materials of the balustrade are two marbles quarried in W-Alps, widely used in historical buildings and monuments in Torino, namely the marble of Prali and the marble of Brossasco. Both are (between others) part of the Palaeozoic marbles belonging to the Dora Maira geological unit (Borghi et al., 2014).

The quarry of Rocca Bianca is located on the NW side of the homonymous mountain, lying in the Dfc zone (D-continental, f-no dy season, c-cold summer; data quantified in the closest monitoring station of Prali, at 1385 m a.s.l.: average temperature ranging from −5.0 °C to 15.0 °C, average annual rainfall around 1400 mm (https://nomadseason.com/climate/italy/piedmont/prali.html). It was the first, historic site of extraction of the marble of Prali, which is perfectly white and composed by medium-grained (0.1–0.8 mm) calcite (95%) with grey veins of mica and chlorite crystals (Borghi et al., 2014; Marini and Mossetti 2006). At present, it has been abandoned for several decades, but still displays extractive walls and quarried blocks, together with ruined buildings and natural outcrops. In the quarry, the marble forms several transposed layers (up to a few metres thick) embedded within micaschists and is characterized by dominant white(-grey) levels alternating with centimetre-thick green dolomite-rich levels (Ghelli 2004). Investigations particularly focused on six, sun-exposed decimetric to metric blocks differing for inclination and lichen community (Fig. 2D–I; blocks 1–6).

2.2. Survey of lithobiontic colonization

Surveys of lichen diversity were carried out on the balustrade of Villa della Regina and in the quarry, finalized to detect dominant species. Lichens were identified on the basis of the online keys published in ITALIC, the Information System of the Italian Lichens, version 07 (see Nimis and Martellos 2020), accessed in autumn 2022. TLC analyses of the secondary metabolites in some thalli followed Orange et al. (2001). Nomenclature of species follows Nimis (2022).

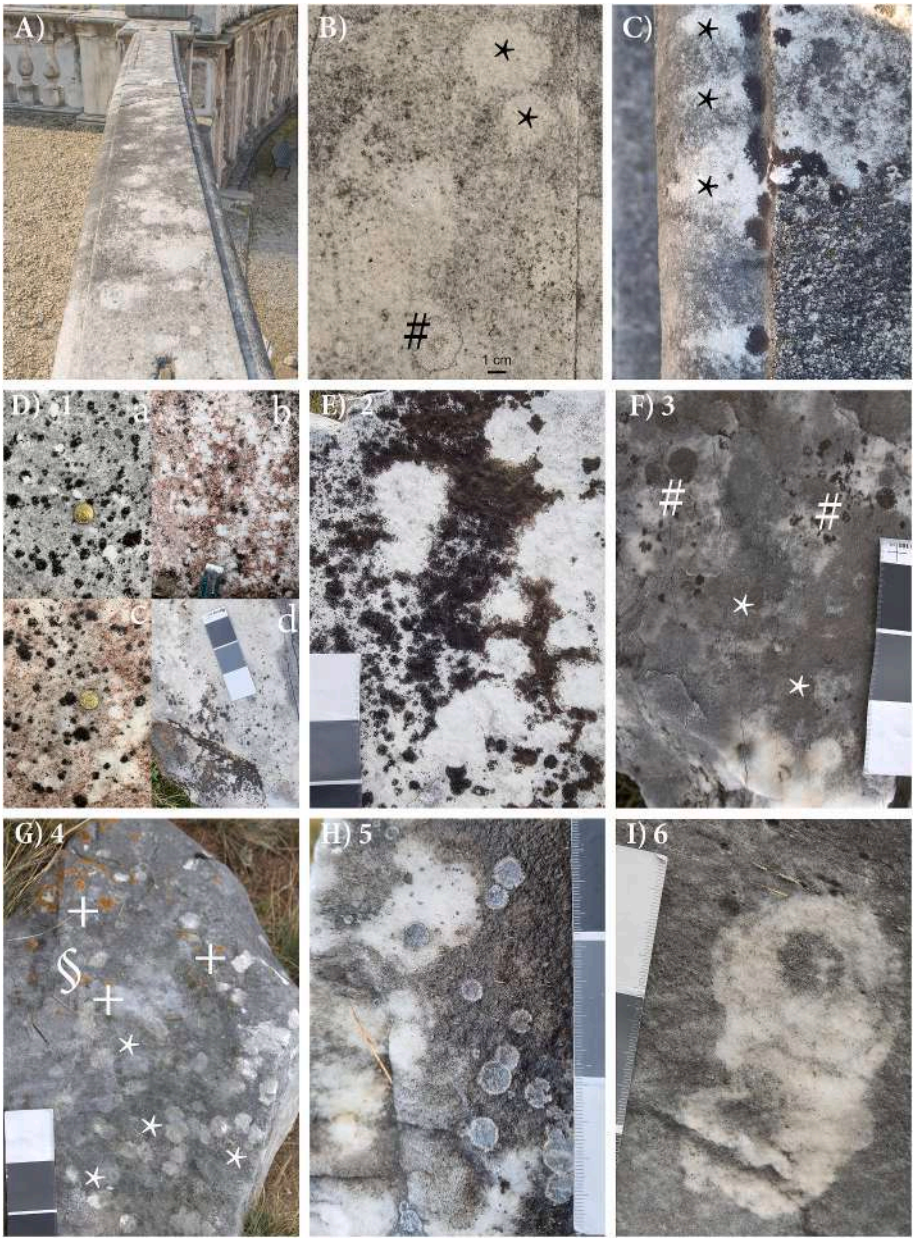

Fig. 2. CUMB patterns on marble surfaces at the Villa della Regina (A–C) and the quarry of Rocca Bianca (D–I). (A) Widespread dark microbial biofilm on a balustrade capstone, interrupted by the presence of CUMBs; (B) CUMBs (*) and a lichen thallus of *Circinaria* gr. *calcarea* of similar dimensions (#); (C) uncolonized areas adjacent to thalli of *Verrucaria macrostoma* in the direction of the water washout from the capstone (*); (D) slightly inclined surfaces of blocks 1a-d with CUMBs and co-occurring brown epilithic thalli of *Staurothele areolata*; (E) block 2, vertical surface with larger CUMBs interposed to a continuous pluricentimetric colonization of the same *S. areolata*; (F) block 3 horizontal surface with CUMBs, small thalli of *S. areolata* (#) surrounded by uncolonized circular borders, and thalli of the endolithic species *Thelidium incavatum* (*); (G) mosaic of CUMBs on the horizontal surface of block 4, mostly colonized by epilithic thalli of *Caloplaca pusilla* (+) and endolithic thalli of *T. incavatum* (*) and, subordinately, *Pyrenodesmia erodens* (§); (H) block 5 horizontal surface with CUMBs, co-occurring thalli of *P. erodens* and a dark microbial biofilm; (I) block 6 vertical surface with CUMBs displaying their center colonized by a dark biofilm.

Biofilms surrounding the CUMBs were also preliminary investigated with regard to their main lithobiontic components, by microscopy observations under a Nikon Eclipse E400.

2.3. Surveys and morphometric characterization of the CUMBs

CUMBs on the balustrade of Villa della Regina were surveyed using an image-analysis approach, particularly focusing on those with diameter higher than 1.5 cm because of their clearly distinguishable appearance at distance. In particular, 6 and 5 capstones were selected for the curved and straight branches of the balustrade, respectively, that is one capstone every three for the curved branch and one every two for the straight one. Digital images (800dpi) were collected using a scanner Epson V10 and the program Epson Scan. They were analyzed by the software WinCam Pro2007d (Regent's Instrument), which quantifies pixels on the basis of color or grey levels, allowing to define the presence and dimension of CUMBs (and lichen thalli), following the protocol proposed by Gazzano et al. (2009). CUMB diameters (or main axis, in the case of non-circular shapes) and circularity were then measured with the program ImageJ (v. 1.46r), operating on the pixel classification image produced by WinCam (Fig. S1).

The same protocol, but images acquired with a Canon EOS 750D, was used to examine CUMBs (and lichen thalli) on the blocks of the abandoned quarry of Rocca Bianca.

A dimensional analysis of lichen thalli was performed for both the sites following the protocol adopted for CUMBs. Dimensions of thalli and CUMBs were compared by means of ANOVA with post-hoc Tukey's test to detect the matrix of pairwise comparison probabilities, using Systat 10.2 (Systat Software Inc., San Jose, CA).

2.4. Physical and mineralogical characterization of the CUMBs

2.4.1. Colorimetric analysis

Colorimetric analyses of CUMBs, and their surrounding surfaces colonized by microbial biofilms, were carried out on the balustrade and on blocks of the quarry of Rocca Bianca. For each of 120 randomly selected CUMBs on the balustrade, from 1 to 5 measures were collected depending on the CUMB size, together with an equal number of

measures from the surrounding surfaces (in total, 425 measures distributed on the 11 selected capstones). With the same approach, a total of 213 measures were collected in the quarry.

Colorimetric measurements were carried out by a portable spectrophotometer (Konica Minolta CM-23d), under the following conditions: geometrical condition d/8 specular component included, D65 illuminant, 2° observer, target area of 8 mm diameter. The data were analyzed by the CIELAB color system (ISO/CIE 11664-4, 2019), evaluating each color by three cartesian or scalar coordinates: L* (lightness, 0–100 black - white); a* (red - green); b* (yellow - blue).

For each group of measures (i.e. CUMB and its colonized surrounding), a ΔE^*_{ab} value was calculated by comparing the average measure obtained on the CUMB with that obtained on the surrounding surfaces colonized by the biofilm (formula 1).

$$\Delta E^*_{ab} = \left[(\overline{L}_C - \overline{L}_B{}^*)^2 + (\overline{a}_C - \overline{a}_B{}^*)^2 + (\overline{b}_C - \overline{b}_B{}^*)^2 \right]^{1/2} \quad (1)$$

Where:

C = CUMB
B = biofilm colonized surfaces

To visualize the L*a*b* color space parameters on a bidimensional plane, a plan (x; y) with the values (L*; a*/b*) was created.

2.4.2. Water absorption analysis

The water absorption (W_a) beneath CUMBs and the surrounding biofilm was evaluated using the contact sponge method, standardized by CEN (EN 17655, 2021). It requires the adoption of a 1034 Rodac plate (23.76 cm^2) containing a natural fiber Calypso sponge produced by Spontex that was imbibed with water to become thicker than the rim of the plate. The sponge was pressed on the stone surface for 1 min and the water absorption was determined by calculating the difference, in mg/cm^2, between the sponge weights measured before and after the contact with the surface (ΔW_a).

In the case of the balustrade, six couple of measurements were carried out in CUMBs ($\Delta W_{a\text{-CUMB}}$) and surrounding colonized areas ($W_{a\text{-bio}}$). In the case of the samples from the quarry of Rocca Bianca, CUMB areas were generally too small to adopt the sponges specifically sold for this test. Accordingly, a natural fiber Calypso sponge produced by Spontex was cut to enter in a cap of a jar with an area of 7.54 cm^2 and pressed on the CUMBs surface for 1 min. Twelves couples of spot measurements were carried out on CUMBs ($\Delta W_{a\text{-CUMB}}$) and in the colonized nearby areas ($W_{a\text{-bio}}$), considered both before and after a gentle cleaning by brush. The difference in water absorption per each couple of measures obtained on the balustrade and the quarry blocks was finally expressed as $\Delta W_{a\text{-CUMB}}/W_{a\text{-bio}}$ ratio.

2.4.3. X-ray powder diffraction analysis

X-ray powder diffraction (XRPD) analyses were performed on sets of samples scraped from randomly selected CUMBs on the balustrade (n = 4) and the quarry blocks (n = 15; block 1, n = 3; block 2, n = 3; block 5, n = 6; block 6, n = 3), their surrounding surfaces colonized by biofilms and/or lichens, and (in the case of the quarry blocks) underneath freshly cut surfaces. In particular, analyses on the balustrade considered the epilithic lichens *Circinaria* gr. *calcarea* (L.) A. Nordin, Savić & Tibell and *Verrucaria macrostoma* DC., and those on the quarry considered the epilithic *Staurothele areolata* (Ach.) Lettau and the endolithic *Pyrenodesmia erodens* (Tretiach, Pinna & Grube) Søchting, Arup & Frödén and *Thelidium incavatum* Mudd. The XRPD patterns were acquired with a Miniflex 600 diffractometer (Rigaku, Tokyo, Japan) operating at 40 kV and 15 mA, using Cu-Kα radiation (λ = 1.5406 Å), in the 2θ range of 3°–70°, scan speed 2°/min with step size 0.02°. Qualitative and semi-quantitative analyses were performed with SmartLab Studio II version 4.3 (Rigaku), using database PDF-4/Minerals 2020, to recognize main phases and peak heights referring to their different crystallographic planes. For each XRPD pattern, the peak height (I, counts) and the full-width at half maximum (FWHM, °) were determined for the main {10–14} and the less intense {01–12} peaks of calcite. In the case of the balustrade, ratios $(I/FWHM)_{Cal\ 01\text{-}12}/(I/FWHM)_{Cal\ 10\text{-}14}$ calculated for CUMBs and lichens were compared with those obtained for the biofilm colonized surfaces (formula 2).

$$\Delta\%\{01-12\}_{balustrade} = \frac{\beta_{C,L}}{\beta_{biofilm}} \quad (2)$$

Where:

$$\beta = \frac{(I/FWHM)_{Cal\ 01-12}}{(I/FWHM)_{Cal\ 10-14}}$$

C = CUMB
L = lichen colonized surfaces.

In the case of the quarry blocks, ratios $(I/FWHM)_{Cal\ 01\text{-}12}/(I/FWHM)_{Cal\ 10\text{-}14}$ calculated for CUMBs, lichen and biofilm colonized surfaces were compared with those obtained for the fresh, unexposed rock volumes (formula 3).

$$\Delta\%\{01-12\}_{block\ n} = \frac{\beta_{C,L,B}}{\beta_{unexposed\ rock}} \quad (3)$$

Where:

block n = quarry blocks 1-6

$$\beta = \frac{(I/FWHM)_{Cal\ 01-12}}{(I/FWHM)_{Cal\ 10-14}}$$

C = CUMB
L = lichen colonized surfaces
B = biofilm colonized surfaces

2.5. UV and microscopic observations of internal stone features

Microscopic observations of cross sections were carried out to investigate the growth of lichens and biofilms within the six blocks of Rocca Bianca, as well as the presence of organic substances in general, and to compare the observed patterns with those detected beneath CUMBs. To accomplish this goal, marble samples of heterogeneous dimensions (l × w × d: 3-40 × 3-30 × 0.5–20 cm) were collected, including lichens and/or CUMBs. Their natural surfaces and those freshly broken by hammer were preliminary observed under long (365 nm) wave UV using a fluorescence analysis cabinet (Model CM-10; Spectroline, Westbury, NY), which could give preliminary insights on the presence of organic substance (Tyson 2012).

A total of 14 polished cross sections were prepared from the blocks, freshly cut with a diamond disk saw. A first set of observations was conducted under optical microscopy in visible light and epifluorescence, using a Nikon Eclipse E400 equipped with two filter blocks, namely, UV-2A (ex 330–380 nm, dm 400, ba 420) and B-2A (ex 450–490, dm 505, ba 520), and a digital camera. Thereafter, the sections were stained with the Periodic acid Schiff's method (Whitlatch and Johnson, 1974), that colours polysaccharides (chitin in the case of the mycobiont partner) inside the stone in shades of magenta, and were observed under a stereomicroscope Olympus SZH. The following parameters were evaluated and quantified: presence and depth of massive hyphal penetration component (i.e. the depth to which hyphae continuously penetrate through intragranular and intergranular voids beneath the whole surface extension of the thallus; *sensu* Favero-Longo et al., 2005, 2009; HD), presence of endolithic biological structures, stained by PAS, not related to a surface lithobiontic cover (deep growths, DG), presence and

thickness of a white opalescent layer (WL), presence and thickness of a dark layer (DL), fluorescence phenomena in the whitish (WF), orange (OF), pink (PF), yellow (YF) and blue (BF) chromatic range. For five selected sections, corresponding thin cross-sections were prepared to run petrographic observations. These were observed using a polarizing microscope equipped with a cathodoluminescence system CITL 8200 mk3 (operating conditions of about 17 kV and 400 μA) in order to search for the potential presence of calcite phases of different origin (Machel, 2000) at the lichen-marble interfaces and in correspondence of the CUMBs.

The results of UV and microscopic observations were finally visualized using a principal coordinate analysis (PCoA) plot (symmetric scaling, centring samples by samples, centring species by species, performed using CANOCO 4.5; Ter Braak and Šmilauer, 2002).

3. Results

3.1. Distribution and morphometry of CUMBs on the marble balustrade and quarried blocks, in comparison with lichens

Image analysis of the marble capstones at the Villa della Regina visualized a total of 960 CUMBs, with a main axis higher than 1.5 cm, that is approx. 80 CUMBs per square meter (Fig. 2A). These were surrounded by a widespread dark microbial biofilm, mainly composed of cyanobacteria and microcolonial fungi (Fig. S2A), and, subordinately, by epilithic crustose lichens, including species with continuous centimetric thalli (*Circinaria* gr. *calcarea* and *Verrucaria macrostoma*) (Fig. 2B and C) and others of lower, (sub-)millimetric dimensions (Table S1). Some of these thalli were locally bordered by biofilm free areas (Fig. S3), which sometimes extended in the direction of water washout (Fig. 2C). It is worth noting that *Circinaria* samples from the balustrade were morphologically identifiable as *C.* gr. *calcarea* (asci with 4 spores, subglobose, 24 × 22 μm; cortex, medulla and apothecium K-; medulla I-), but, on the basis of TLC, they lacked aspicilin. As expected, *V. macrostoma* did not exhibit lichen secondary metabolites.

Image analysis showed that CUMBs on the balustrade had a major axis in the range 1.7–8.2 cm (Fig. 3A), with highest frequency of CUMBs with major axis between 2.0 and 4.0 cm (51%; dispersion of data detailed in Fig. S4). The median circularity (ratio of the main axes) of CUMBs was 1.3 (central quartiles comprised between 1.1 and 1.6; 5–95 percentiles between 1.0 and 2.9), indicating a rather circular size (Fig. 3C). With respect to the lichen thalli, the median major axis, and the circularity ratio of *C.* gr. *calcarea* were 2.2 cm and 1.2, respectively, while in the case of *V. macrostoma* they were 1.1 cm and 1.3, respectively. *Candelariella aurella* (Hoffm.) Zahlbr. and *Myriolecis* gr. *dispersa* (Pers.) Sliwa, Zhao Xin & Lumbsch were widespread on the balustrade,

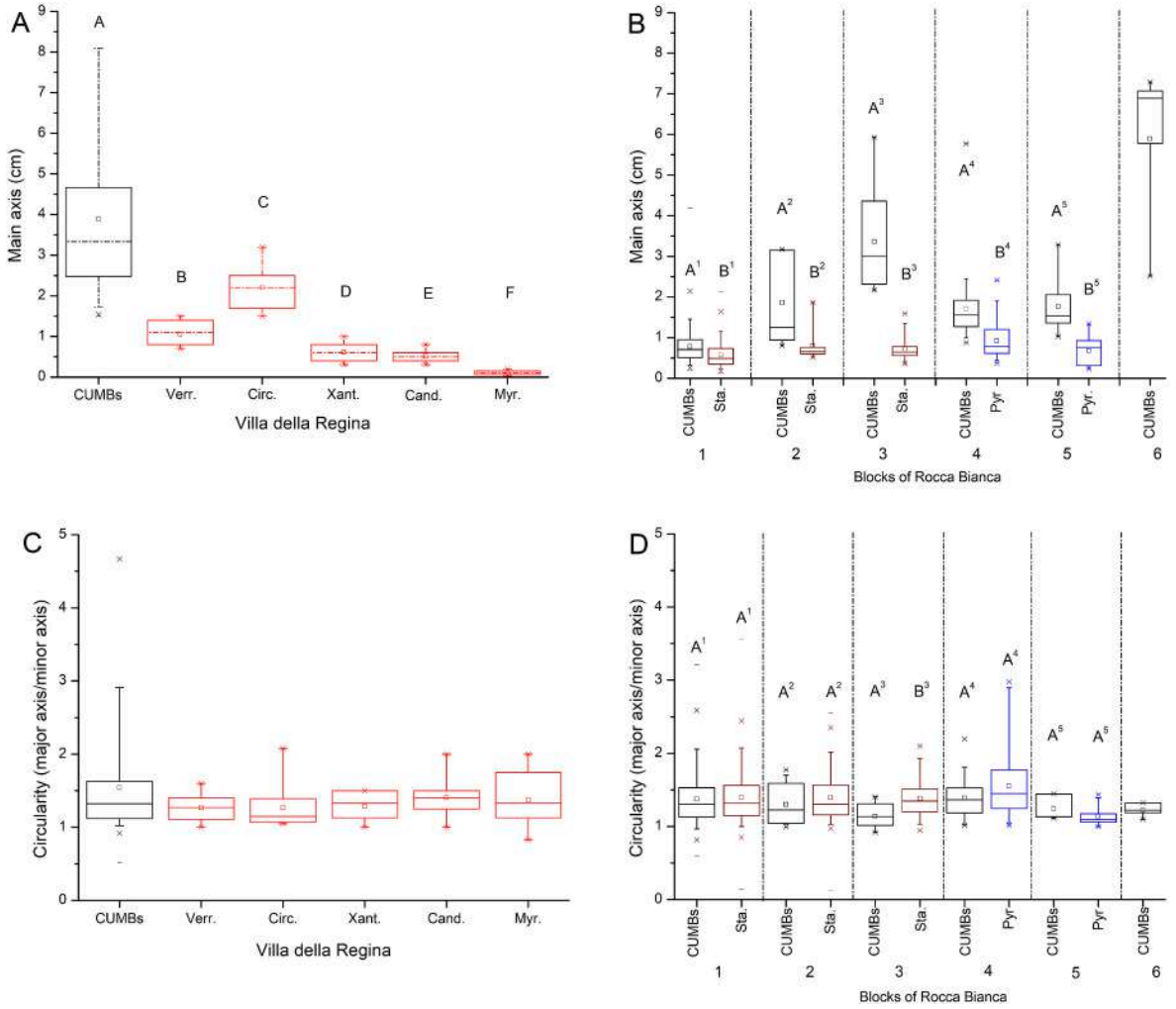

Fig. 3. Morphometric analysis (length of main axis, A-B, and circularity, C-D) of CUMBs and lichens on (A, C) the balustrade at the Villa della Regina (Verr, *Verrucaria macrostoma*; Circ, *Circinaria* gr. *calcarea*; Xant, *Xanthocarpia crenulatella*; Cand, *Candelariella aurella*; Myr, *Myriolecis dispersa*) and (B, D) at the quarry of Rocca Bianca, separately considered for blocks 1–6 (blocks 1–3, Sta, *Staurothele areolata*; 4–5, Pyr, *Pyrenodesmia erodens*). Boxplots show 95th percentile (upper whisker), 75th percentile (top box), median (transversal line), mean (small square), 25th percentile (bottom box), 5th percentile (lower whisker). With reference to the balustrade and per each block of the quarry, box-plots not sharing at least one letter are significantly different (ANOVA with Tukey's post-hoc test, $p < 0.05$).

and *Xanthocarpia crenulatella* (Nyl.) Frödén, Arup & Søchting locally occurred, but they all displayed small thalli (av. main axis <0.5 cm).

The survey in the quarry of Rocca Bianca similarly showed marble surfaces displaying co-presence of microbial biofilm (Fig. S2B), CUMBs and lichens (blocks 1–5; Fig. 2D–H), and also a block, free of lichens, with CUMBs with uncolonized circular borders and the colonized center, similar to those described by Caneva et al. (2020) (block 6; Fig. 2I). Lichen communities associated with the CUMBs on the different examined blocks included epilithic crustose species of genera *Staurothele* and *Calogaya*, and endolithic species of genera *Thelidium* and *Pyrenodesmia* (Table S1, with details on the different blocks). On these blocks, a total of 680 CUMBs was quantified. Their frequency was strongly different on the different blocks, ranging between approx. 70 (block 1a) to 0.5 (blocks 3 and 6) per square decimeter, and was significantly proportional to the number of lichen thalli on the same surfaces ($R^2 = 0.91$; $p < 0.01$; Fig. S5). The species of the family Verrucariaceae observed on the examined marble surfaces lack lichen secondary metabolites, while, in the case of Teloschistaceae, the epilithic *Calogaya pusilla* (A. Massal.) Arup, Frödén & Søchting produces antraquinones and the endolithic *Pyrenodesmia erodens* produces *Sedifolia*-grey pigments.

Measures of CUMBs and associated lichens in the quarry of Rocca Bianca are separately reported for the examined blocks (Fig. 3B). On blocks 1-2-4-5, the dimensional range of CUMBs and lichens partially overlapped, with the former being always slightly, but significantly wider, while CUMBs were strongly wider than lichens on block 3. On blocks 1a-d, 2, and 3 (Fig. 2D–F), CUMBs with main axis ranging from av. 0.7–3.2 cm were placed between distinct thalli of *Staurothele areolata* with diameters of av. 0.6–0.7 cm (blocks 1, Fig. 2D; block 3, Fig. 2F) or contiguous ones, determining a continuous pluricentimetric colonization (block 2, Fig. 2E). Some thalli of irregular shape due to a partial detachment of areolae made visible the substrate (Fig. 2Da), and or were surrounded by uncolonized circular borders (Fig. 2F), with patterns resembling that of the adjacent CUMBs. CUMBs and lichens also coexisted on blocks 4 and 5, characterized by epilithic thalli of *Calogaya pusilla* and endolithic thalli of *Thelidium incavatum* and *Pyrenodesmia erodens*, with 5–95 percentiles between 0.3 and 1.8 cm, observed both surrounded by a dark microbial biofilm and in the middle of CUMBs (Fig. 2G and H). On blocks 1, 2, 4 and 5, the circularity of CUMBs did not significantly differ from that of lichens, while it was lower in the case of block 3 (Fig. 3D). Few larger CUMBs, with an average main axis of 6 cm were observed on the vertical surface of block 6, covered by a dark microbial biofilm for the rest and free of lichens (Fig. 2I). These CUMBs were peculiarly colonized by the biofilm in their central part.

3.2. Physical modifications of the stone material in CUMBs and mineralogical investigation

The colorimetric analysis of the CUMBs on the balustrade quantified the colour difference with respect to the nearby biofilm-colonized areas (ΔE^*_{ab} 20.11 ± 1.77), and data showed that this was due to a difference in Lightness (L*), while a*/b* ratio was similar (Fig. 4A). In particular, L* was significantly lower in the case of surfaces colonized by the microbial biofilm. A similar pattern of L* values was quantified at the Rocca Bianca quarry, where the fresh cut stone showed even higher values than the CUMBs and a slightly lower a*/b* ratio (due to slightly higher b* values; not shown), although shifts were minimal (Fig. 4B).

CUMBs displayed a lower absorption with respect to the nearby areas covered by the biofilm, on both the balustrade (median $\Delta W_{a\text{-CUMB}}/W_{a\text{-bio}} = 0.75$, with 5–95 percentiles in the range 0.55–0.85) and the blocks sampled from the quarry of Rocca Bianca (median $W_{a\text{-CUMB}}/W_{a\text{-bio}} = 0.8$ with 5–95 percentiles in the range 0.5–0.9) (Fig. 5). In the case of these latter, however, the ratio was inverted when the measures were repeated after the biofilm removal (median $W_{a\text{-CUMB}}/W_{a\text{-bio}} = 1.4$ with 5–95 percentiles in the range 1.05–2.1).

X-ray diffraction of balustrade samples showed some higher presence of calcite with stabilization of the calcite {01–12} form in correspondence of CUMBs with respect to the nearby areas colonized by biofilms. In Fig. 6A, such pattern is shown by positive values of percentage difference (+45%) between the $(I/FWHM)_{Cal\ 01\text{-}12}/(I/FWHM)_{Cal\ 10\text{-}14}$ ratios calculated for the CUMBs and the nearby areas colonized by biofilms. Such positive percentage difference was also detected (+55%) by comparing samples collected beneath *C. calcarea* with the biofilm colonized areas (Fig. S6), while similar $(I/FWHM)_{Cal\ 01\text{-}12}/(I/FWHM)_{Cal\ 10\text{-}14}$ ratios were displayed by *V. macrostoma* and the biofilm.

In the case of samples from the quarry, $(I/FWHM)_{Cal\ 01\text{-}12}/(I/FWHM)_{Cal\ 10\text{-}14}$ calculated for each block for CUMBs, biofilms and/or lichens were compared with those obtained for fresh unexposed volumes

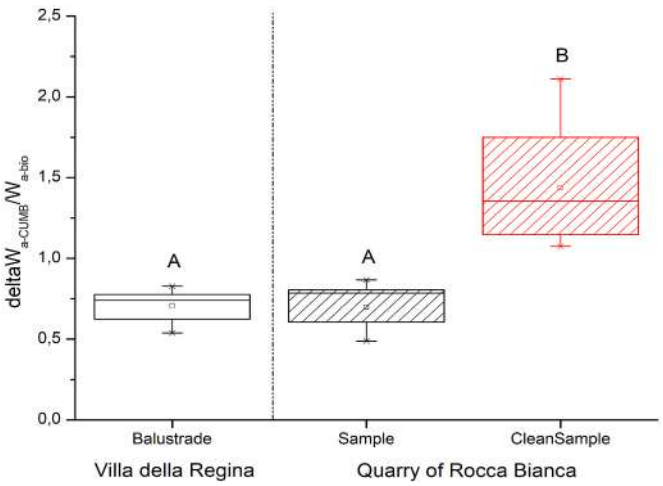

Fig. 5. Water absorption in correspondence of the CUMBs and the surrounding colonized areas, expressed as ratio between the two values (black boxplots). In the case of the quarry, the measures were repeated after the cleaning of the biofilm (red boxplot). Values shown by box-plots as in Fig. 3; box-plots not sharing at least one letter are significantly different (ANOVA with Tukey's post-hoc test, $p < 0.05$).

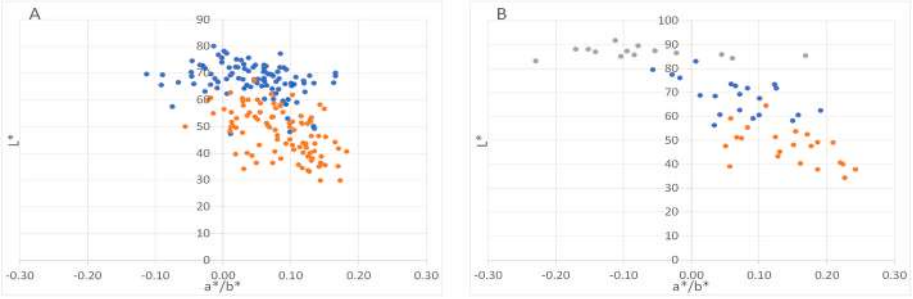

Fig. 4. Lightness (L*) and a*/b* ratios of CUMBs (blue dots) and their biofilm colonized surrounding areas (orange dots) on (A) the balustrade of Villa della Regina and on (B) the marble blocks of the quarry of Rocca Bianca. For the quarry blocks, measures obtained from freshly cut surfaces are also reported (grey dots).

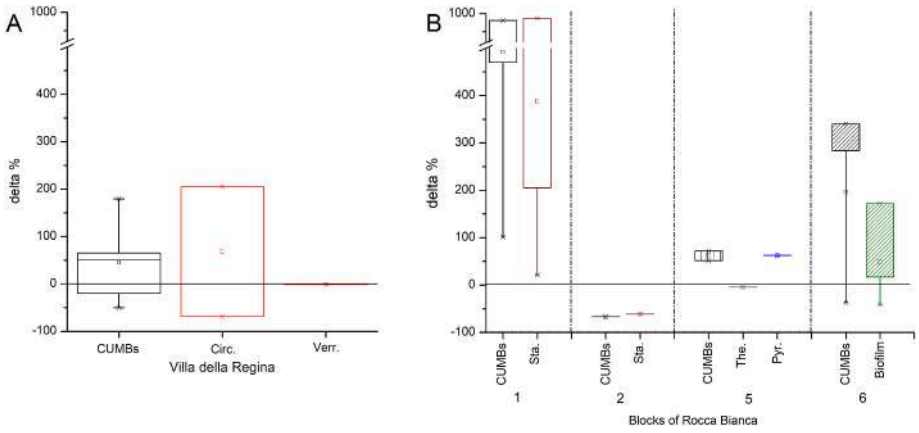

Fig. 6. XRPD analyses. (A) percentage difference between the $(I/FWHM)_{Cal\ 01\text{-}12}/(I/FWHM)_{Cal\ 10\text{-}14}$ ratios calculated for the CUMBs and the lichens (Circ, *Circinaria calcarea*; Verr, *Verrucaria macrostoma*) with respect to the nearby areas colonized by biofilms; (B) percentage difference between the $(I/FWHM)_{Cal\ 01\text{-}12}/(I/FWHM)_{Cal\ 10\text{-}14}$ ratios calculated for the CUMBs and the different blocks (1 and 2. *Staurothele areolata*; 5 *Thelidium incavatum* and *Pyrenodesmia erodens*; 6. biofilm) with respect to the fresh unexposed stone. Values shown by box-plots as in Fig. 3.

(Fig. 6B). CUMBs on blocks 6 and 1 displayed relatively higher percentage differences (av. approx. +200% and +500%) with respect to the fresh controls in comparison with the biofilm (+50%) and *Staurothele areolata* (+400%), respectively. In the case of block 5, CUMBs and *P. erodens* displayed positive percentage differences (approx. +50%) of $(I/FWHM)_{Cal\ 01\text{-}12}/(I/FWHM)_{Cal\ 10\text{-}14}$ ratios with respect to the fresh control, while *T. incavatum* displayed similar values. Only in the case of block 2, a negative percentage difference of $(I/FWHM)_{Cal\ 01\text{-}12}/(I/FWHM)_{Cal\ 10\text{-}14}$ ratios was observed with respect to fresh controls for both the CUMBs and the large thalli of *S. areolata*.

Oxalates were not found in correspondence of any CUMB, but only beneath *Circinaria* thalli on the balustrade.

3.3. Stone features and biological structures beneath CUMBs, in comparison with biofilms and lichens

The marble samples collected in the quarry and observed under UV light and by fluorescence microscopy displayed remarkable autofluorescence phenomena both at their surface and the (sub-)millimetric layers beneath it, exposed in the polished cross sections. Besides the chlorophyll red autofluorescence, associated to epilithic and endolithic lichen photobionts and some phototrophic components of biofilms, orange, pinkish-orange, yellow, and whitish autofluorescences were observed in correspondence of both CUMBs and/or nearby colonized areas, although clear patterns were hardly recognizable. In particular, orange fluorescence was observed on the surface and in the depth (down to 5 mm) of block 6, in correspondence of the biofilm surrounding the CUMBs (Fig. S7A), while these latter did not show the same pattern (Fig. S7C). Whitish, pinkish-orange and yellowish fluorescence -extended from the surface to the upper layers of the rock- characterized CUMBs interposed between the grey endolithic thalli of *P. erodens* and *T. incavatum* on blocks 5 (Fig. S7E), and in the proximity of thalli of *C. pusilla* and the biofilm on block 4, respectively. On blocks 1, pinkish fluorescence characterized some, but not all, CUMBs and thalli of *S. areolata* (Fig. S7G), which were not associated to fluorescence phenomena on block 2.

PAS staining of the cross sections, representative of the different quarry blocks, did not stain the CUMBs surfaces and did not visualize any remarkable penetration of biological structures beneath them. Except for blocks 3 and 4, an uncolonized, white opalescent layer from the CUMB surface down to 0.5–3.0 mm was a common trait (Fig. S7D). Only in some cases, a dark band (block 6) and/or deep hyphal growths (blocks 1, 2, 5, 6) were observed beneath this opalescent layer. Microscopical observation of the colonized areas surrounding the CUMBs displayed microbial growth from the surface down to a depth of 6 mm. In some samples, a dark band was also observed at this depth (Fig. S7B). The white opalescent layer was observed with a lower frequency beneath the biofilm of block 6 and also of block 4, where it was not present beneath the CUMBs.

All lichens exhibited a hyphal penetration component developing within the rock, but with different spread and depth depending on the species. *P. erodens* displayed pervasive hyphal penetration within small channels perpendicular to the surface down to 0.3 mm, with thin hyphae locally extending to higher depths, down to 5.5 mm (Fig. S7F). *T. incavatum* massively penetrated the marble down to 0.5 mm, with a sparse penetration of thin hyphae being locally observed down to 1.3 mm. The epilithic *S. areolata* showed a pervasive penetration in the case of large thalli on blocks 2 and 3, with hyphal bundles widespread within the mineral substrate down to 2.0 mm, and thin hyphae diffusely penetrating down to 8.0 mm. The smaller thalli of the same species on block 1 only displayed a similar network of thin hyphae, penetrating down to a maximum of 5.7 mm (Fig. S7H). A white opalescent layer, similar to that observed beneath CUMBs, was observed immediately beneath the endolithic thalli on block 5 and *S. areolata* on blocks 1, 2 and 3. A darker band parallel to the surface was also observed in the case of blocks 2, 3 (large thalli of *S. areolata*) and 5 (*P. erodens*).

In all cases, cathodoluminescence microscopy observation on thin cross sections obtained from the same blocks observed under fluorescence and light microscopy (and examined with XRPD) did not detect differences in surface and deep rock layers, including those displaying the various fluorescence phenomena, potentially informative on calcite phases of different origin (Fig. S8).

The PCoA, which extracted four main axes explaining 97.5% of total variance, summarizes in Fig. 7 the variability registered by the UV and microscopic observations. Hyphal penetration depth (HD), dark layer thickness (DL) and orange fluorescence (OF) were positively related to the first (46.9% of total variance), second (29.4%) and third (14.0%) axes, respectively. Deep growths (DG, that is the presence of PAS-stained structures beginning only from deep layers) was negatively correlated to the first axis, while white layer (WL) and whitish fluorescence (WF) showed negative correlations with all the three axes. Most of CUMBs clustered in the third quadrant, positively related to DG and WL, although some of them also scattered along the second axis, related to DL. *S. areolata* and *P. erodens* mostly scattered in the lower quadrants, displaying higher positive correlation with HD than *T. incavatum*. This latter mostly scattered in the left side of the diagram, showing a high correlation with both WF and WL along the third axis. Biofilm samples were heterogeneously distributed along the first axis, in some cases showing positive correlation with the DL and the OF along the second and third axes, respectively. Yellow, pink and blue fluorescence (YF, PF, BF) were superimposed in the third quadrant oppositely to HD and DL, likely driven by their limited number of reports. Although some clustering of samples obtained from each block was detected, this appeared subordinate to the described patterns related to different lithobionts and CUMBs.

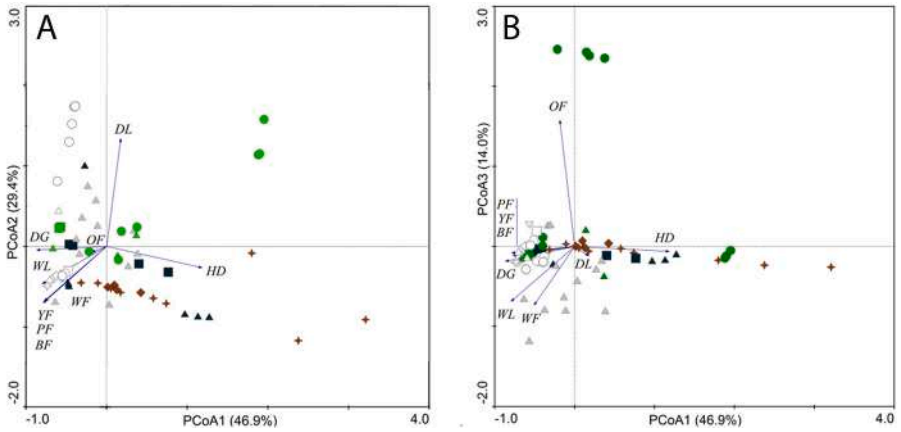

Fig. 7. Ordination of cross-sectioned samples prepared from blocks 1–6 of the Rocca Bianca quarry on the basis of different parameters quantified by microscopic and UV observations (A, axes 1 and 2; B, axes 1 and 3). Samples are marked according to different lithobionts (biofilm, green symbols; *Staurothele areolata*, brown; *Pyrenodesmia erodens*, blue; *Thelidium incavatum*, grey) and CUMBs (white), and blocks (1, diamond; 2, star; 3, square; 4, down-triangle; 5, up-triangle; 6, circle). HD, hyphal penetration depth; DG, deep growths; WL, white opalescent layer; DL, dark layer; WF, whitish, OF, orange, PF, pink, YF, yellow, and BF, blue fluorescences.

4. Discussion

At the best of our knowledge, glossaries internationally accepted as official references in the framework of Cultural Heritage conservation (e.g., Vergès-Belmin, 2008) do not include any dedicated term and description for the centimetric circular areas persistently free from epilithic microbial growths, that we examined here under the term of CUMBs. As previously shown, they can be the case of absence of natural colonization (as in the quarry) or recolonization following restoration interventions (as for the Villa della Regina). Although colorimetric results (Fig. 4) may qualify CUMBs as discolorations (i.e. changes of rock colour, *sensu* Vergès-Belmin, 2008), they result from the absence of a surrounding microbial deterioration pattern, and may even represent bioprotection features. Nevertheless, their characterization and that of the causes of these differential bioreceptivity patterns appear worth to be considered. Their relevance arises not only for the need of better qualify the visual features of stone surfaces, giving useful nomenclatures for communication issue, but also for the potential clue to address innovative strategies to avoid recolonization processes following restoration.

In this work, we provided a first morphometric characterization of CUMBs on a marble, and we verified their distributional and dimensional compatibility with lichens (re-)colonizing surfaces in their vicinity, both on a heritage structure and in the original quarry site, now representing a semi-natural condition. Moreover, invasive analyses on quarry materials displayed, for marble layers immediately beneath CUMBs and lithobionts, several modified patterns with respect to the fresh rock, including chromatic shifts and fluorescence, together with variously organized, penetrating biological structures. A high variability occurred in the association of these phenomena with CUMBs, the microbial biofilm and different lichen species, also depending on the considered blocks. However, CUMBs were mostly associated with the absence of penetrating structures immediately beneath the rock surface, where a white opalescent layer was a common trait. Such pattern was related with a higher presence of calcite displaying the stabilization of the {01–12} calcite form, which is favoured by the presence of organic substances (Pastero et al., 2003), in comparison with the fresh rock. Such phenomenon was shared by several lichen-colonized samples, supporting the hypothesis of a CUMBs-lichens relationship. In the following sub-sections, we discuss these findings, summarized in Table S2, focusing on the elements of compatibility between CUMBs and lichens and on features potentially informative on the CUMBs origin.

4.1. Distributional and dimensional compatibility of CUMBs and lichens

Investigations on lithobiontic colonization of natural marble surfaces, exposed following a glacier retreat, showed rock-dwelling fungi, algae and cyanobacteria preceding the colonization by lichens (Hoppert et al., 2004). Similarly, microbial biofilms are earlier colonizers than lichens on carbonate heritage surfaces (Hoppert and König, 2006; Caneva et al., 2008; Pinheiro et al., 2019). For algae and cyanobacterial, few years after a treatment can be sufficient to a wide recolonization (Delgado Rodrigues et al., 2011; Bartoli et al., 2021). In the case of the balustrade of Villa della Regina, considered about twenty years after the last restoration, the darkening (av. $L^* = 47.6$) due to the biofilm thoroughly affected its surface, sparing CUMBs only, while lichen colonization was less widespread. Lichenometric studies, aiming to date minimal surface exposure on the basis of lichen size, particularly focused on longevity and mortality rates of the species more frequently used for this practical application. In the case of *Rhizocarpon geographicum*, annual mortality rates between 0.4% and 5.1% of thalli were reported for different sites, indicating a relatively low turnover of individuals in natural populations (Osborn et al., 2015). Cleaning interventions by restorers radically change this scenario, with a simultaneous removal of all thalli. With this regard, if lichens may leave tracks of their colonization, these should be simultaneously appreciable on surfaces which underwent restoration activity. The tracks should instead cyclically appear on natural surfaces, likely resulting more sporadically, although these patterns would also generally depend on the initial abundance of thalli. Accordingly, the high frequency of CUMBs on the marble balustrade would suggest a high lichen colonization before the cleaning intervention at the beginning of 2000s, but, unfortunately, the photographic documentation, although highlighting the widespread biological colonization on the heritage surface, was not oriented to detail the presence and distribution of the different lithobionts (Fig. S9). On the other hand, with respect to the quarry surfaces, high heterogeneity of CUMBs frequency observed on the blocks was significantly correlated with that of lichen thalli (Fig. S5). Such link between lichen colonization and CUMBs may appear at odds with the detected dimensional divergence, with thalli significantly larger than the uncolonized areas on the same surface. However, on both the balustrade and the quarry blocks, CUMBs major axis appeared partially superimposed to maxima values of lichen thalli (with the exception of block 3). With this regard, it is worth noting that thalli measured on the balustrade are relatively young, as their recolonization, even if immediately started after the cleaning, dates back approx. twenty years, while thalli possibly occurring before the cleaning could be at a more mature growth stage. Similarly, in the case of the quarry, maxima dimensions of the thalli may be expected to correspond to their final stage of development, associated with decreased growth rates, senescence, and, possibly, final detachment of the dead parts (Armstrong and Bradwell, 2010; Osborn et al., 2015), and thus account for a further pattern of relationship with CUMBs. On the rocks hosting many small thalli (*S. areolata* on blocks 1), CUMBs also display highest density and minimal dimensions. Moreover, centimetric bare areas surrounding saxicolous crustose lichens were reported in literature and related to the allelopathic potential of lichen secondary

metabolites, although few experiments have supported these field observations (Armstrong and Welch, 2007). Similar clean surfaces were also observed on the balustrade, around well-developed thalli of *Verrucaria* and *Circinaria* (Fig. S3). However, they were more likely related to re-growths of the same species on surfaces they already occupied before the cleaning, and from which they were not effectively removed, than to inhibitory halos. Indeed, these phenomena were not thoroughly observed around all individuals, *V. macrostoma* does not produce secondary lichen metabolites (Nimis 2022) and *C.* gr. *calcarea* lacked aspicilin in the examined site. In the same context, the central parts of senescent thalli were shown to degenerate, determining the formation of 'windows' available for new colonization by the same or other species (Armstrong and Welch, 2007). The phenomenon was also observed in the case of senescent thalli of *C. calcarea* (Pentecost, 1980). Similar patterns may also justify colonization of black biofilms in the center of some larger CUMBs, as those observed on the Caestia Pyramid (Caneva et al., 2020), on the balustrade and in the case of block 6, although on the latter no lichen presence was observed.

4.2. Microscopical and mineralogical features pointing to a CUMB - lichen relationships due to stone physical modifications or allelopathic effects

Colonization by biofilms and lichens also affects the marble interior, as observed on PAS-stained sections from the quarry. The development of the hyphal penetration component (*sensu* Favero-Longo et al., 2005) of lichens within marbles down to millimetric depths was widely reported in literature (e.g., Hoppert et al., 2004; Garvie et al., 2008). In the examined material, the values of massive and maximum penetration (*sensu* Favero-Longo et al., 2005, 2009) of *S. areolata*, down to 2.0 and 8.0 mm, respectively, were higher than the ranges of 0.3–0.7 mm and 1.0–3.0 mm, depending on the marble, reported for other epilithic species of Verrucariaceae, as *Verrucaria nigrescens* and *V. macrostoma* (Favero-Longo et al., 2009). Although the penetration of *Circinaria* gr. *calcarea* within the balustrade could not be examined, it is worth noting that depths of massive and maximum penetration within marble in the range 0.4–1.0 mm were reported for other species of the genus (*Circinaria contorta*; Modenesi and Lajolo, 1988). A pattern of massive hyphal penetration down to 0.3 mm and 0.5 mm, respectively, combined with a strongly deeper network of thin hyphae down to several millimeters, also characterized the endolithic *P. erodens* and *T. incavatum*. In particular, the development of vertical channels by *P. erodens* was analogously observed for the species within limestone (Pinna and Salvadori, 2000). The same ranges of penetration were observed for *Thelidium absconditum* within Carrara marble (Workgroup 'Cultural Heritage' of Lichen Italian Society, unpublished data). In all cases, penetration depths and hyphal spread appeared lower than those observed for the same or phylogenetically related species within limestone (Fry, 1922; Pinna et al., 1998; Matteucci et al., 2019; Tonon et al., 2022). Within the examined substrate, hyphal penetration was indeed limited to a sparse intercrystalline penetration driven by the intrinsic textural properties, in particular the medium-grained calcite, as already observed for species of genus *Verrucaria* colonizing other poorly porous marbles (Favero-Longo et al., 2009). Similarly, the penetration of *C. contorta* within marble was shown to exploit preexisting porosity between crystals, leaving an impression on calcite crystals, but not penetrating them (Modenesi and Lajolo, 1988).

On the other hand, some hyphae and other PAS-stained biological structures were also observed at deep layers, independent from lichen occurrences at the surface (i.e. also in correspondence of CUMBs and biofilm), according to the high spread and diversity of lithobionts growing endolithically characterized by molecular studies for marbles and other lithologies (Bjelland and Ekman, 2005; Bjelland et al., 2011; Sajjad et al., 2022). The characterization of such diversity of deep penetrating structures go beyond the interest of this work and will be part of a subsequent paper. Nevertheless, the widespread biological structures observed within the marble down to several millimeters of depth particularly remarked the peculiarity of the absence of PAS-staining down to several hundreds of microns beneath the CUMBs. In depth heavy growths contrasting low level of superficial colonization were observed in volcanic rocks of an archaeological site, several decades after their treatment with biocides, and evaluated as residues of previous colonizers (Caneva et al., 2005). In the case of the marble quarry, the low colonization of CUMB surface rock layers (i.e. the opalescent layer) at least in some blocks was followed by deep growths. Such observation indicates for CUMBs a lower bioreceptivity not only at the marble surface, but also related to the upper internal layers of the rock, suggesting some differences in intrinsic properties which may favor or not the microbial colonization and penetration with respect to other areas. Accordingly, Caneva et al. (2020) hypothesized that uncolonized circular areas on the Caestia Pyramid may be related to a modification in the physical rock properties or to the long-lasting presence of allelopathic substances. However, the production of secondary metabolites was not a trait of the Verrucariaceae on the balustrade and the quarry blocks, showing a dimensional compatibility with the CUMBs, and also *Circinaria* gr. *calcarea* at Villa della Regina did not display the production of aspicilin considered by Caneva et al. (2020) as a possible inhibitory agent on the Pyramid. On the other hand, the opalescent layer displayed by CUMBs as a common trait was also observed beneath lichens, while rarely shared by the biofilm colonized surfaces (visualized in the PCoA by the positive relation of the WL vector with CUMBs and most of lichens, opposed to biofilm marks). Similarly, color shifts, associated or not to the loss of original textural features, were previously observed by some of us in the upper layers of other carbonate rocks, namely the Portland and Botticino limestones, when colonized by lichens, and putatively associated to their biogeochemical activity (Morando et al., 2017). Other modifications of limestones colonized by lichens have been also associated with an endolithic dissolution of calcite and the entrapment of organic matter beneath the surface, determining some bioprotective effects (Concha-Lozano et al., 2012). More in general, endolithic lichens were shown to determine a reprecipitation of fine-grained calcite, building a protective coat on the colonized surfaces (Garvie et al., 2008). A similar process was not microscopically observed for the examined marble, even by cathodoluminescent investigations which could potentially discriminate calcites precipitated in different conditions (Machel, 2000). However, XRPD analyses of calcite scraped from CUMBs and lichens similarly showed some higher stabilization of the {01–12} form with respect to biofilm colonized areas on the balustrade and fresh controls representative of quarry blocks (with the exception of block 2). This behavior has been particularly associated to calcite crystallization in presence of organic chelants (Pastero et al., 2003; Tonon et al., 2022), providing some correlation of its higher frequency with biogeochemical processes.

Calcite dissolution and reprecipitation by lichens, including euendolithic ones (actively dissolving calcite *sensu* Golubic et al., 1981), have been associated to different processes, including a respiration-induced process only (Weber et al., 2011), but patterns are still not generally understood (Pinna, 2021). Biogenic concretions after lichen thalli died were associated to remains of oxalates (and carbonates) entrapping organic and mineral matter (Ariño et al., 1995). In the case of the examined surfaces, oxalates were only detected in the XRPD analyses performed beneath the *C.* gr. *calcarea* on the balustrade. The release of the common lichen-secreted chelant oxalic acid is not typically associated to the endolithic *P. erodens* (Pinna and Salvadori, 2000) and the epilithic and endolithic Verrucariaceae (Pinna et al., 1998), except for *Verrucaria rubrocincta* (Bungartz and Garvie, 2004). However, aposymbiotic cultures of some endolithic lichen species of Verrucariaceae demonstrated the production of iron chelating molecules *in vitro* (Favero-Longo et al., 2011). On the other hand, both calcicolous epilithic species of genus *Circinaria* and endolithic Verrucariaceae are known to produce oil hyphae, which were the object of pioneer microscopic observations (Fry, 1922) and subsequent chemical

characterization of their lipid contents (Kushnir et al., 1978), but their role has been not fully explained and was not connected with lichen biodeterioration activities until now (Salvadori and Casanova Municchia, 2016; Jung and Büdel, 2021). However, as reported in the case of the alga *Acutodesmus obliquus* (Natsi and Koutsoukos, 2022), a high concentration of lipids may increase the concentration of carboxylic groups within the substrate, creating additional growth sites for calcite. With this regard, Modenesi and Lajolo (1988) microscopically documented the capillary presence of oil droplets in the hyphae of *C. contorta* penetrating within marble along its intercrystalline discontinuities. Although we did not investigate the presence of oil hyphae, this mentioned literature provides some support to the hypothesis that the hyphal penetration component of lichens can provide the organic compounds responsible for the stabilization of the calcite {01–12} form during a reprecipitation process. How the cleaning operations, by removing the thalli and their photobiont later, may promote such hypothesized process and, thus, further relate with CUMBs is worth of future investigations.

Biological reprecipitation processes were related to bioprotective effects, due to the development of surface coatings and the closure of discontinuities between mineral grains, reducing substrate porosity (Gadd and Dyer, 2017). Despite the hyphal penetration, lichen cover can determine an unmodified or even reduced water absorption by different lithic substrates, until the thalli are not mechanically removed from the surfaces, reverting the pattern (Morando et al., 2017; Pinna et al., 2023). The performed absorption tests agreed with this latter scenario, with CUMBs absorbing more water than the nearby colonized surfaces (considered after the biofilm removal). This observation supports the hypothesis that a previous lichen penetration could have increased the substrate porosity by their physical action (Modenesi and Lajolo, 1988; Garvie et al., 2008; Favero-Longo et al., 2009), while leaves unresolved the reasons of the lower bioreceptivity, which contrasts with the higher water availability within the substrate (Sanmartín et al., 2021).

The presence of organic matter within carbonate rocks was associated to the observation of fluorescence phenomena (Tyson, 2012). These were limited to the upper rock layers, thus ruling out a correlation with general impurities of the examined marble, and rather addressing a surface-localized concentration related to the presence of lithobionts. If Verrucariaceae are not producers of lichen secondary metabolites, often associated to autofluorescence under UV light (Orange et al., 2001), *C. pusilla* and *P. erodens* are known to produce antraquinones, which can have allelopathic functions (Gazzano et al., 2013), and the related alternative pigment *Sedifolia*-grey, respectively (Nimis, 2022). However, fluorescence phenomena were also variously associated to the microbial biofilm on block 6, *S. areolata* on block 1, and other CUMBs, preventing a direct correlation with a certain lithobiontic component and the CUMBs (visualized in the PCoA by the superimposed orientation of all the fluorescence vectors in the third quadrant). Other approaches are thus necessary to target the potential presence of allelopathic substances entrapped in the reprecipitated calcite, according to the hypothesis by Caneva et al. (2020). With this regard, Raman spectroscopy already allowed the detection of secondary metabolites as biomarkers of past colonization of rocks by lichens (Casanova Municchia et al., 2014), and thus appears a promising approach for future steps of this research. Nevertheless, it is also worth noting that successive generations of different lithobionts may potentially superimpose their effects and metabolite traces, justifying the complex detected scenario (Morando et al., 2017).

In the analyzed case, a CUMBs-lichens relationship is thus suggested by some microscopical and mineralogical features (first of all calcite reprecipitation and the whitish opalescent layer beneath both lichens and CUMBs), together with field evidence of frequent co-presence and a morphometric and distributional compatibility. It is worth remembering that the CUMBs phenomenon was here examined on surfaces in different climatic zones (Köppen-Geiger Cfa and Dfc zones), but sharing, as common conditions, an exposure to direct sun irradiation and the marble lithology. Further investigations are necessary to extend the comprehension of ecological conditions associated to the lichen-origin of such CUMBs phenomenon and the differences with those connected with other causative factors (see Fig. 1).

5. Conclusion

This work characterized centimetric circular areas left free from biofilm (re-)colonization on marble surfaces of both cultural heritage and quarry sites, showing elements of morphometric, distributional, microscopical and mineralogical compatibility with tracks of a past lichen colonization. In particular, CUMBs and lichen colonized surfaces shared evidences of calcite reprecipitation, that may affect physical properties of the upper internal layers of the rock and, thus, their bioreceptivity. However, observations also indicated a surface-localized concentration of organic matter, which is worth of further spectroscopic investigations to evaluate the potential occurrence of allelopathic compounds. Clarifying an effective combination of physical modification and enrichment in bioactive molecules of the surface marble layers may drive the implementation of innovative strategies to prevent recolonization of stone cultural heritage.

Declaration of competing interest

The authors declare that they have no known competing financial interests or personal relationships that could have appeared to influence the work reported in this paper.

Data availability

Data will be made available on request.

Acknowledgements

This study was funded by University of Torino grants (RiLo). The authors are grateful to Alessandra Guerrini, Laura Moro, and Chiara Teolato (Direzione Regionale Musei Piemonte, previously Polo Museale del Piemonte) for permission to access the Villa della Regina for this study, and to all the personnel of the monumental site for logistic support. Moreover, the authors thank Enrica Matteucci, Mariagrazia Morando, Greta Rao Torres, Alessia Romano, Silvia Sciacca, Chiara Tonon (University of Torino) and Paola Iacomussi (INRIM) for assistance during some phases of fieldwork and helpful discussions, and two anonymous reviewers for their valuable suggestions to improve the clarity of the manuscript.

Appendix A. Supplementary data

Supplementary data to this article can be found online at https://doi.org/10.1016/j.ibiod.2023.105681.

References

Ariño, X., Ortega-Calvo, J.J., Gomez-Bolea, A., Saiz-Jimenez, C., 1995. Lichen colonization of the roman pavement at baelo claudia (cadiz, Spain): biodeterioration vs. bioprotection. Sci. Total Environ. 167, 353–363. https://doi.org/10.1016/0048-9697(95)04595-R.

Armstrong, R.A., Welch, A.R., 2007. Competition in lichen communities. Symbiosis 43, 1–12.

Armstrong, R., Bradwell, T., 2010. Growth of crustose lichens: a review. Geogr. Ann. Phys. Geogr. 92, 3–17. https://doi.org/10.1111/j.1468-0459.2010.00374.x.

Bartoli, F., Casanova Municchia, A., Futagami, Y., Kashiwadani, H., Moon, K.H., Caneva, G., 2014. Biological colonization patterns on the ruins of Angkor temples (Cambodia) in the biodeterioration vs bioprotection debate. Int. Biodeterior. Biodegrad. 96, 157–165. https://doi.org/10.1016/j.ibiod.2014.09.015.

Bartoli, F., Casanova Municchia, A., Leotta, M., Luciano, S., Caneva, G., 2021. Biological recolonization dynamics: kentridge's artwork disappearing along the Tiber embankments (Rome, Italy). Int. Biodeterior. Biodegrad. 160, 105214 https://doi.org/10.1016/j.ibiod.2021.105214.

Bjelland, T., Ekman, S., 2005. Fungal diversity in rock beneath a crustose lichen as revealed by molecular markers. Microb. Ecol. 49, 598–603. https://doi.org/10.1007/s00248-004-0101-z.

Bjelland, T., Grube, M., Hoem, S., Jorgensen, S.L., Daae, F.L., Thorseth, I.H., Øvreås, L., 2011. Microbial metacommunities in the lichen–rock habitat. Environ. Microbiol. Rep. 3, 434–442. https://doi.org/10.1111/j.1758-2229.2010.00206.x.

Borghi, A., d'Atri, A., Martire, L., Castelli, D., Costa, E., Dino, G., Favero Longo, S.E., Ferrando, L., Gallo, M., Giardino, M., Groppo, C., Piervittori, R., Rolfo, F., Rossetti, P., Vaggelli, G., 2014. Fragments of the Western Alpine chain as historic ornamental stones in Turin (Italy): enhancement of urban geological heritage through geotourism. Geoheritage 6, 41–55. https://doi.org/10.1007/s12371-013-0091-7.

Bungartz, F., Garvie, L.A., 2004. Anatomy of the endolithic Sonoran Desert lichen *Verrucaria rubrocincta* Breuss: implications for biodeterioration and biomineralization. Lichenol. 36, 55–73. https://doi.org/10.1017/S0024282904013854.

Caneva, G., Salvadori, O., Ricci, S., Ceschin, S., 2005. Ecological analysis and biodeterioration processes over time at the Hieroglyphic Stairway in the Copán (Honduras) archaeological site. Plant Biosyst. 139, 295–310. https://doi.org/10.1080/11263500500343353.

Caneva, G., Nugari, M.P., Salvadori, O. (Eds.), 2008. Plant Biology for Cultural Heritage: Biodeterioration and Conservation. Getty Publications.

Caneva, G., Lombardozzi, V., Ceschin, S., Casanova Municchia, A., Salvadori, O., 2014. Unusual differential erosion related to the presence of endolithic microorganisms (Martvili, Georgia). J. Cult. Herit. 15, 538–545. https://doi.org/10.1016/j.culher.2013.10.003.

Caneva, G., Fidanza, M.R., Tonon, C., Favero-Longo, S.E., 2020. Biodeterioration patterns and their interpretation for potential applications to stone conservation: a hypothesis from allelopathic inhibitory effects of lichens on the Caestia Pyramid (Rome). Sustainability 12, 1132. https://doi.org/10.3390/su12031132.

Carter, N.E.A., Viles, H.A., 2005. Bioprotection explored: the story of a little-known earth surface process. Geomorphology 67, 273–281. https://doi.org/10.1016/j.geomorph.2004.10.004.

Casanova Municchia, A., Caneva, G., Ricci, M.A., Sodo, A., 2014. Identification of endolithic traces on stone monuments and natural outcrops: preliminary evidences. J. Raman Spectrosc. 45, 1180–1185. https://doi.org/10.1002/jrs.4517.

Chen, J., Blume, H.P., Beyer, L., 2000. Weathering of rocks induced by lichen colonization—a review. Catena 39, 121–146. https://doi.org/10.1016/S0341-8162(99)00085-5.

Concha-Lozano, N., Gaudon, P., Pages, J., De Billerbeck, G., Lafon, D., Eterradossi, O., 2012. Protective effect of endolithic fungal hyphae on oolitic limestone buildings. J. Cult. Herit. 13, 120–127. https://doi.org/10.1016/j.culher.2011.07.006.

Cuberos-Cáceres, L., Calvo-Bayo, I., Romero-Noguera, J., Bolivar-Galiano, F., 2022. Study and development of a new methods to inhibit the growth of biofilm in the ornamental fountains of the Alhambra and the Generalife. In: Di Martino, P., Cappitelli, F., Villa, F., Bruno, L. (Eds.), ECBSM 2022-European Conference on Biodeterioration of Stone Monuments, fifth ed., p. 36.

Danin, A., Caneva, G., 1990. Deterioration of limestone walls in Jerusalem and marble monuments in Rome caused by cyanobacteria and cyanophilous lichens. Int. Biodeterior. 26, 397–417. https://doi.org/10.1016/0265-3036(90)90004-Q.

Delgado Rodrigues, J., Anjos, M.V., Charola, A.E., 2011. Recolonization of marble sculptures in a garden environment. In: Charola, A.E., McNamara, C., Koestler, R. (Eds.), Biocolonization of Stone: Control and Preventive Methods. Smithsonian Contributions to Museum Conservation, vol. 2. Smithsonian Institution Scholarly Press, Washington, pp. 71–85.

de los Ríos, A., Souza-Egipsy, V., 2021. The interface of rocks and microorganisms. In: Burkhard Büdel, B., Friedl, T. (Eds.), Life at Rock Surfaces. De Gruyter, Berlin, pp. 3–38. https://doi.org/10.1515/9783110646467.

Dyer, T., 2017. Deterioration of stone and concrete exposed to bird excreta examination of the role of glyoxylic acid. Int. Biodeterior. Biodegrad. 125, 125–141. https://doi.org/10.1016/j.ibiod.2017.09.002.

Edwards, H.G., Seaward, M.R., Attwood, S.J., Little, S.J., de Oliveira, L.F., Tretiach, M., 2003. FT-Raman spectroscopy of lichens on dolomitic rocks: an assessment of metal oxalate formation. Analyst 128 (10), 1218–1221. https://doi.org/10.1039/B306991P.

EN 17655, 2021. Conservation of Cultural Heritage - Determination of Water Absorption by Contact Sponge Method.

Favero-Longo, S.E., Castelli, D., Salvadori, O., Belluso, E., Piervittori, R., 2005. Pedogenetic action of the lichens *Lecidea atrobrunnea, Rhizocarpon geographicum* gr. and *Sporastatia testudinea* on serpentinized ultramafic rocks in an alpine environment. Int. Biodeterior. Biodegrad. 56, 17–27. https://doi.org/10.1016/j.ibiod.2004.11.006.

Favero-Longo, S.E., Borghi, A., Tretiach, M., Piervittori, R., 2009. In vitro receptivity of carbonate rocks to endolithic lichen-forming aposymbionts. Mycol. Res. 113, 1216–1227. https://doi.org/10.1016/j.mycres.2009.08.006.

Favero-Longo, S.E., Gazzano, C., Girlanda, M., Castelli, D., Tretiach, M., Baiocchi, C., Piervittori, R., 2011. Physical and chemical deterioration of silicate and carbonate rocks by meristematic microcolonial fungi and endolithic lichens (Chaetothyriomycetidae). Geomicrobiol. J. 28, 732–744. https://doi.org/10.1080/01490451.2010.517696.

Favero-Longo, S.E., Viles, H.A., 2020. A review of the nature, role and control of lithobionts on stone cultural heritage: weighing-up and managing biodeterioration and bioprotection. World J. Microbiol. Biotechnol. 36, 7. https://doi.org/10.1007/s11274-020-02878-3.

Fry, E.J., 1922. Some types of endolithic limestone lichens. Ann. Bot. 36, 541–562.

Gadd, G.M., 2017. Geomicrobiology of the built environment. Nat. Microbiol. 2, 1–9. https://doi.org/10.1038/nmicrobiol.2016.275.

Gadd, G.M., Dyer, T.D., 2017. Bioprotection of the built environment and cultural heritage. Microb. Biotechnol. 10, 1152–1156. https://doi.org/10.1111/1751-7915.12750.

Garvie, L.A., Knauth, L.P., Bungartz, F., Klonowski, S., Nash, T.H., 2008. Life in extreme environments: survival strategy of the endolithic desert lichen Verrucaria rubrocincta. Naturwissenschaften 95, 705–712. https://doi.org/10.1007/s00114-008-0373-0.

Gazzano, C., Favero-Longo, S.E., Matteucci, E., Piervittori, R., 2009. Image analysis for measuring lichen colonization on and within stonework. Lichenol. 41, 299–313. https://doi.org/10.1017/S0024282909008366.

Gazzano, C., Favero-Longo, S.E., Iacomussi, P., Piervittori, R., 2013. Biocidal effect of lichen secondary metabolites against rock-dwelling microcolonial fungi, cyanobacteria and green algae. Int. Biodeterior. Biodegrad. 84, 300–306. https://doi.org/10.1016/j.ibiod.2012.05.033.

Ghelli, A., 2004. Marmi di Rocca Bianca. Tra particolarità litologiche e sapiente sfruttamento antropico. In: Aigotti, D. (Ed.), I geositi nel paesaggio alpino della Provincia di Torino, vol. 1. Litografia Geda di Nichelino, Torino, pp. 75–80.

Golubic, S., Friedmann, E.I., Schneider, J., 1981. The lithobiontic ecological niche, with special reference to microorganisms. J. Sediment. Res. 51, 475–478. https://doi.org/10.1306/212F7CB6-2B24-11D7-8648000102C1865D.

Guglielmin, M., Favero-Longo, S.E., Cannone, N., Piervittori, R., Strini, A., 2011. Role of lichens in granite weathering in cold and arid environments of continental Antarctica. Geol. Soc. Spec. Publ. 354, 195–204. https://doi.org/10.1144/SP354.12.

Guillitte, O., 1995. Bioreceptivity: a new concept for building ecology studies. Sci. Total Environ. 167, 215–220. https://doi.org/10.1016/0048-9697(95)04582-L.

Hoppert, M., Flies, C., Pohl, W., Günzl, B., Schneider, J., 2004. Colonization strategies of lithobiontic microorganisms on carbonate rocks. Environ. Geol. 46, 421–428. https://doi.org/10.1007/s00254-004-1043-y.

Hoppert, M., König, S., 2006. The succession of biofilms on building stone and its possible impact on biogenic weathering. Heritage, Weather. Conserv. 2, 311–315.

ISO/CIE 11664-4, 2019. Colorimetry — Part 4: CIE 1976 L*a*b* Colour Space.

Jung, P., Büdel, B., 2021. Lichens as pioneers on rock surfaces. In: Burkhard Büdel, B., Friedl, T. (Eds.), Life at Rock Surfaces. De Gruyter, Berlin, pp. 141–160. https://doi.org/10.1515/9783110646467.

Kottek, M., Grieser, J., Beck, C., Rudolf, B., Rubel, F., 2006. World map of the Köppen-Geiger climate classification updated. Meteorol. Z. 15, 259–263. https://doi.org/10.1127/0941-2948/2006/0130.

Kushnir, E., Tietz, A., Galun, M., 1978. "Oil hyphae" of endolithic lichens and their fatty acid composition. Protoplasma 97, 47–60. https://doi.org/10.1007/BF01276389.

Lombardozzi, V., Castrignanò, T., D'Antonio, M., Casanova Municchia, A., Caneva, G., 2012. An interactive database for an ecological analysis of stone biopitting. Int. Biodeterior. Biodegrad. 73, 8–15. https://doi.org/10.1016/j.ibiod.2012.04.016.

Machel, H.G., 2000. Application of cathodoluminescence to carbonate diagenesis. In: Pagel, M., Barbin, V., Blanc, P., Ohnenstetter, D. (Eds.), Catodoluminescence in Geosciences. Springer, Berlin, Heidelberg, pp. 271–302. https://doi.org/10.1007/978-3-662-04086-7_11.

Marini, P., Mossetti, C., 2006. Natural stones used in a royal House of piedmont (Italy). In: Fort, R., Alvarez de Buergo, M., Gomez-Heras, M., Vazquesz-Calvo, M. (Eds.), Proceedings of the International Conference on Heritage, Weathering and Conservation, vol. 2. Taylor & Francis Group, London, pp. 895–900.

Matteucci, E., Scarcella, A.V., Croveri, P., Marengo, A., Borghi, A., Benelli, C., Hamdan, O., Favero-Longo, S.E., 2019. Lichens and other lithobionts on the carbonate rock surfaces of the heritage site of the tomb of Lazarus (Palestinian territories): diversity, biodeterioration, and control issues in a semi-arid environment. Ann. Microbiol. 69, 1033–1046. https://doi.org/10.1007/s13213-019-01465-8.

McIlroy de la Rosa, J.P., Warke, P.A., Smith, B.J., 2013. Lichen-induced biomodification of calcareous surfaces: bioprotection versus biodeterioration. Prog. Phys. Geogr. 37, 325–351. https://doi.org/10.1177/0309133312467660.

McIlroy de la Rosa, J.P., Warke, P.A., Smith, B.J., 2014. The effects of lichen cover upon the rate of solutional weathering of limestone. Geomorphology 220, 81–92. https://doi.org/10.1016/j.geomorph.2014.05.030.

Miralles, I., Edwards, H.G., Domingo, F., Jorge-Villar, S.E., 2015. Lichens around the world: a comprehensive study of lichen survival biostrategies detected by Raman spectroscopy. Anal. Methods 7, 6856–6868. https://doi.org/10.1039/C5AY00655D.

Modenesi, P., Lajolo, L., 1988. Microscopical Investigation on a Marble Encrusting Lichen, vol. 8. Studia Geobotanica, pp. 47–64.

Morando, M., Wilhelm, K., Matteucci, E., Martire, L., Piervittori, R., Viles, H.A., Favero Longo, S.E., 2017. The influence of structural organization of epilithic and endolithic lichens on limestone weathering. Earth Surf. Process. Landforms 42, 1666–1679. https://doi.org/10.1002/esp.4118.

Natsi, P.D., Koutsoukos, P.G., 2022. Calcium carbonate mineralization of microalgae. Biomimetics 7, 140. https://doi.org/10.3390/biomimetics7040140.

Nimis, P.L., 2022. ITALIC - the Information System on Italian Lichens. University of Trieste, Dept. of Biology. Version 7.0. https://dryades.units.it/italic, 2022, 12.

Nimis, P.L., Martellos, S., 2020. Towards a digital key to the lichens of Italy. Symbiosis 82, 149–155. https://doi.org/10.1007/s13199-020-00714-8.

Nimis, P.L., Pinna, D., Salvadori, O., 1992. Licheni e conservazione dei monumenti. CLU Editrice, Bologna, Italy.

Orange, A., James, P.W., White, F.J., 2001. Microchemical Methods for the Identification of Lichens. British Lichen Society.

Osborn, G., McCarthy, D., LaBrie, A., Burke, R., 2015. Lichenometric dating: science or pseudo-science? Quat. Res. 83, 1–12. https://doi.org/10.1016/j.yqres.2014.09.006.

Pastero, L., Costa, E., Alessandria, B., Rubbo, M., Aquilano, D., 2003. The competition between {1014} cleavage and {0112} steep rhombohedra in gel grown calcite crystals. J. Cryst. Growth 247, 472–482. https://doi.org/10.1016/S0022-0248(02)01911-5.

Pentecost, A., 1980. Aspects of competition in saxicolous lichen communities. Lichenol. 12, 135–144. https://doi.org/10.1017/S0024282980000060.

Piervittori, R., Salvadori, O., Seaward, M.R.D., 2004. Lichens and monuments. In: St Clair, L.L., Seaward, M.R.D. (Eds.), Biodeterioration of Stone Surfaces. Lichens and Biofilms as Weathering Agents of Rocks and Cultural Heritage. Kluwer Academic Publishers, Dordrecht, pp. 241–282. https://doi.org/10.1007/978-1-4020-2845-8_2.

Pinheiro, A.C., Mesquita, N., Trovão, J., Soares, F., Tiago, I., Coelho, C., de Carvalho, H. P., Gil, F., Catarino, L., Piñar, G., Portugal, A., 2019. Limestone biodeterioration: a review on the Portuguese cultural heritage scenario. J. Cult. Herit. 36, 275–285. https://doi.org/10.1016/j.culher.2018.07.008.

Pinna, D., Salvadori, O., Tretiach, M., 1998. An anatomical investigation of calcicolous endolithic lichens from the Trieste karst (NE Italy). Plant Biosyst. 132, 183–195. https://doi.org/10.1080/11263504.1998.10654203.

Pinna, D., Salvadori, O., 2000. Endolithic lichens and conservation: an underestimated question. In: Fassina, V. (Ed.), Proceedings of the 9th International Conference on Deterioration and Conservation of Stone, vol. 1. Elsevier, Amsterdam, pp. 513–519. https://doi.org/10.1016/B978-044450517-0/50136-7.

Pinna, D., 2021. Microbial growth and its effects on inorganic heritage materials. In: Joseph, E. (Ed.), Microorganisms in the Deterioration and Preservation of Cultural Heritage. Springer Nature, pp. 3–35. https://doi.org/10.1007/978-3-030-69411-1.

Pinna, D., Mazzotti, V., Gualtieri, S., Voyron, S., Andreotti, A., Favero-Longo, S.E., 2023. Damaging and protective interactions of lichens and biofilms on ceramic dolia and sculptures of the International Museum of Ceramics, Faenza, Italy. Sci. Total Environ. 877, 162607 https://doi.org/10.1016/j.scitotenv.2023.162607.

Sajjad, W., Ilahi, N., Kang, S., Bahadur, A., Zada, S., Iqbal, A., 2022. Endolithic microbes of rocks, their community, function and survival strategies. Int. Biodeterior. Biodegrad. 169, 105387 https://doi.org/10.1016/j.ibiod.2022.105387.

Salvadori, O., Casanova Municchia, A., 2016. The role of fungi and lichens in the biodeterioration of stone monuments. Open Conf. Proc. J. 7, 39–54. https://doi.org/10.2174/2210289201607020039.

Sanmartín, P., Miller, A.Z., Prieto, B., Viles, H.A., 2021. Revisiting and reanalysing the concept of bioreceptivity 25 years on. Sci. Total Environ. 770, 145314 https://doi.org/10.1016/j.scitotenv.2021.145314.

Seaward, M.R., 2015. Lichens as agents of biodeterioration. Recent Adv. Lichenol.: Mod. Method. Approach. Biomonitor. Bioprospect. 1, 189–211. https://doi.org/10.1007/978-81-322-2181-4_9.

Slavík, M., Bruthans, J., Filippi, M., Schweigstillová, J., Falteisek, L., Řihošek, J., 2017. Biologically-initiated rock crust on sandstone: mechanical and hydraulic properties and resistance to erosion. Geomorphology 278, 298–313. https://doi.org/10.1016/j.geomorph.2016.09.040.

Ter Braak, C.J.F., Šmilauer, P., 2002. CANOCO Reference Manual and CanoDraw for Windows User's Guide: Software for Canonical Community Ordination. Microcomputer Power, Ithaca, NY, p. 500, version 4.5.

Tonon, C., Bernasconi, D., Martire, L., Pastero, L., Viles, H., Favero-Longo, S.E., 2022. Lichen impact on sandstone hardness is species-specific. Earth Surf. Process. Landforms 47, 1147–1156. https://doi.org/10.1002/esp.5307.

Tyson, R.V., 2012. Sedimentary Organic Matter: Organic Facies and Palynofacies. Springer Science & Business Media.

Vergès-Belmin, V., 2008. Illustrated glossary on stone deterioration patterns. Icomos.

Weber, B., Scherr, C., Bicker, F., Friedl, T., Büdel, B., 2011. Respiration induced weathering patterns of two endolithically growing lichens. Geobiology 9, 34–43. https://doi.org/10.1111/j.1472-4669.2010.00256.x.

Whitlatch, R.B., Johnson, R.G., 1974. Methods for staining organic matter in marine sediments. J. Sediment. Res. 44, 1310–1312. https://doi.org/10.1306/212F6CAD-2B24-11D7-8648000102C1865D.